

The Galactic bulge millisecond pulsars shining in X rays: A γ -ray perspective

Joanna Berteaud,^{1,*} Francesca Calore,^{1,†} Maïca Clavel,² Pasquale Dario Serpico,¹ Guillaume Dubus,² and Pierre-Olivier Petrucci²

¹*Univ. Grenoble Alpes, USMB, CNRS, LAPTh, F-74940 Annecy, France*

²*Univ. Grenoble Alpes, CNRS, IPAG, F-38000 Grenoble, France*

(Dated: June 7, 2022)

If the mysterious Fermi-LAT GeV γ -ray excess is due to an unresolved population of millisecond pulsars (MSP) in the Galactic bulge, one expects this very same population to shine in X rays. For the first time, we address the question of what is the sensitivity of current X-ray telescopes to an MSP population in the Galactic bulge. To this end, we create a synthetic population of Galactic MSPs, building on an empirical connection between γ - and X-ray MSP emission based on observed source properties. We compare our model with compact sources in the latest *Chandra* source catalog, applying selections based on spectral observables and optical astrometry with *Gaia*. We find a significant number of *Chandra* sources in the region of interest to be consistent with being bulge MSPs that are as yet unidentified. This motivates dedicated multi-wavelength searches for bulge MSPs: Some promising directions are briefly discussed.

Introduction. A mysterious excess, discovered at GeV energies in the data of the Large Area Telescope (LAT) onboard the *Fermi* satellite, has been thrilling scientists for more than a decade. The so-called *Fermi* GeV excess has been thoroughly characterized by several, independent, groups, see e.g. [1–5]. Its spectral energy distribution is peaked at about 2 GeV, resembling the cumulative emission of known millisecond pulsars (MSPs) [6] or what is expected from dark matter particles annihilating into high-energy photons [7]. Its spatial distribution, instead, traces old stars in the Galactic bulge more closely than what is predicted from dark matter annihilation models [8, 9]. These findings support the hypothesis that the excess is caused by a large population of MSP-like γ -ray emitters in the Galactic bulge, too faint to be detected as individual sources by the LAT (i.e. *unresolved*). Early analyses of photon counts statistics [10, 11] appeared to corroborate these conclusions, but the dark matter interpretation has been revamped recently [12, 13], because of yet unexplored systematics affecting photon counts statistical methods [14–16].

To conclusively prove the nature of the *Fermi* GeV excess, a multi-wavelength approach can allow us to test (and constrain) the “unresolved MSPs” hypothesis. Predictions for radio observations with current and future telescopes [17] have contributed to propel an on-going observational effort with radio interferometers, such as the Very Large Array (VLA) and MeerKAT, to look for radio counterparts of the *Fermi* GeV excess. Future multi-messenger probes involving gravitational waves have also been discussed [18]. For sure, MSPs also emit X rays through thermal (from heating of magnetic polar caps) or non-thermal (e.g. from relativistic particle acceleration in the pulsar magnetosphere, or shock-driven interactions between pulsar wind and companion material in

binaries) mechanisms [19]. Several X-ray analyses have targeted known radio and/or γ -ray MSPs to look for X-ray counterparts, e.g. [20–22]. The most complete census of known X-ray MSPs [22] spectrally characterized about 50 MSPs with data from *Chandra*, *XMM-Newton*, *Suzaku*, *Swift*, *ROSAT*, and *BeppoSAX*.

Building on the multi-wavelength emission of MSPs, here we assess *for the first time* what is the sensitivity of current X-ray telescopes, notably *Chandra*, to a Galactic bulge MSP population which would be responsible for the *Fermi* GeV excess. While γ -ray data are not sensitive yet to the detection of individual bulge MSPs [23, 24], *can the available deep X-ray observations of the inner Galaxy unveil them?* To answer this question, we create a synthetic population of Galactic MSPs, which includes contribution from an MSP bulge component modeled such as to match spatial and spectral observations of the GeV excess. X-ray predictions are inferred via an empirical connection between γ - and X-ray MSP emission based on [22]. We then discuss X-ray spectral cuts as well as the complementary information provided by *Gaia* astrometric observations. The goal is to understand how far we are from a possible discovery and, anticipating our encouraging findings, to promote dedicated multi-wavelength searches for bulge MSPs.

The Galactic MSP population. We consider the Galactic MSPs to be composed by an observationally rather well-constrained disk component, plus the elusive population in the Galactic bulge, putative origin of the *Fermi* GeV excess.

The γ -ray population modeling. We base the modeling of Galactic MSPs on γ -ray observations. The MSP disk spatial distribution and γ -ray luminosity function (GLF) are obtained from the analysis of 96 *Fermi*-LAT identified γ -ray MSPs [23]. We adopt the “Lorimer-disk” best-fit spatial distribution and the best-fit broken power-law GLF (see App. A). Following the best-fit results of [23], the total number of disk MSPs is about 24000.

* berteaud@lapth.cnrs.fr

† calore@lapth.cnrs.fr

The spatial distribution of bulge MSPs builds upon the results of [8], and follows the morphology of red clump giants in the boxy bulge (BB) [25] and of infrared observations of the nuclear bulge (NB) [26] (more details provided in App. A). Although it is difficult to constrain the GLF of bulge MSPs due to the lack of resolved γ -ray objects, existing studies have found that it could be consistent with the GLF of resolved disk MSPs [27, 28]. We therefore assume the GLF of bulge MSPs to be the same as the one for the disk population. We will show that our predictions are only mildly affected by changes of the GLF parameters. Fixing the GLF and imposing that the total average luminosity of the Galactic bulge component matches the best-fit estimates from [8], the total number of sources in the BB and NB are found to be 27674 and 2700, respectively. From GLF and source spatial distribution, we can then simulate a corresponding γ -ray energy flux for each synthetic source in the 0.1 – 100 GeV band.

The X-ray flux distribution. Many studies exist on the correlation between X-ray and γ -ray luminosities and pulsars’ spin-down power, see e.g [29–31]. However, in order to predict X-ray fluxes of our synthetic sources, we rely on the empirical connection between observed γ - and X-ray MSP emission properties. Ref. [22] presents power-law spectral fits to 47 detected X-ray MSPs, 40 of which we found to have γ -ray counterparts in the latest release of the 4FGL catalogue [32].

The number of MSPs emitting in γ rays and the one emitting in X rays may differ, for instance due to the different (and poorly constrained) emission geometries [21]. Based on the calibration sample, to the purpose of an X-ray prediction it is however *conservative* to assume that each γ -ray MSP in our Monte Carlo simulation also has associated X-ray emission, an hypothesis that we make in the following. Thus, we compute the γ -to-X flux ratio F_γ/F_X of the 40 X-ray MSPs having γ -ray counterpart, where F_γ is the 0.1 – 100 GeV energy flux and F_X the 0.2 – 10 keV *unabsorbed* energy flux.

The other variable of interest is the X-ray spectral index, Γ , provided by [22]. Since Γ is significantly correlated with $\log_{10}(F_\gamma/F_X)$ (Spearman coefficient of 0.782), we build a 2D probability distribution function (PDF) of $\log_{10}(F_\gamma/F_X)$ and Γ from the 40 MSPs. Given the paucity of data, we use a kernel density estimation (KDE) algorithm [33] to derive the joint PDF, checking the stability of the result against the bandwidth choice and the optimization algorithm. From this PDF, displayed in Fig. 1, we extract an F_γ/F_X ratio and index Γ for each synthetic source. Knowing F_γ for each synthetic source, we can then generate a corresponding X-ray flux. On the other hand, extracting X-ray spectral indices for our simulated sources allows us to model F_X in any energy band, in particular the ones covered by *Chandra*.

The *absorbed* differential photon flux per unit of energy

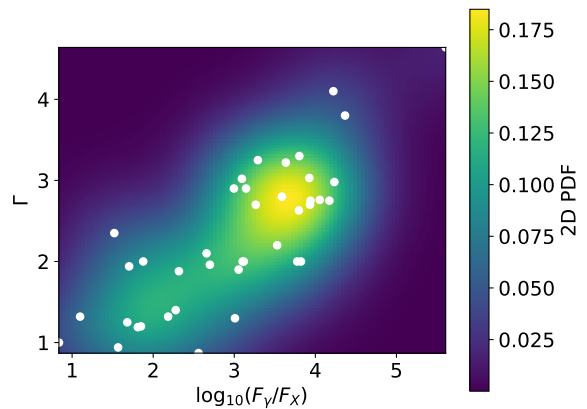


FIG. 1. KDE 2D joint PDF (colored background) of $\log_{10}(F_\gamma/F_X)$ and X-ray spectral index Γ from the 40 X-ray observed MSPs having a γ -ray counterpart. Original data from [22] are shown by the white dots.

is obtained by modeling the Galactic absorption:

$$\begin{aligned} S^{\text{abs}}(E) &= S^{\text{unabs}}(E) \times \exp(-N_H \sigma(E)) \\ &= A (E/1 \text{ keV})^{-\Gamma} \times \exp(-N_H \sigma(E)), \end{aligned} \quad (1)$$

where $S^{\text{unabs}}(E)$ is the unabsorbed photon flux, modelled by a power law with amplitude A and spectral index Γ . N_H (cm^{-2}) is the total hydrogen column density along the line of sight, and $\sigma(E)$ the photoelectric absorption cross section. We parameterize $\sigma(E)$ as in [34] with Galactic elemental abundances from [35]. To build the hydrogen column density N_H , we use the publicly available gas maps adopted in [9]. These maps are obtained from atomic (HI) and molecular (HII) hydrogen surveys [36, 37] with an hydrodynamic approach, which accounts for non-circular gas motion in the inner Galaxy. Since hydrodynamic maps have better kinematic resolution towards the inner Galaxy, we adopt those as baseline hydrogen model. They are split in four concentric rings, providing a coarse-grained 3D hydrogen distribution. The total column density being $N_H = N_{\text{HI}} + 2N_{\text{HII}} + N_{\text{dust}}$, we also include the contribution from the dark neutral medium [38] by using the residuals reddening maps from [9]. We test other choices for the modeling of the total hydrogen column density in App. B.

Comparison with *Chandra* catalog. With its unique high spatial resolution and low instrumental background, *Chandra* is an excellent instrument to image the X-ray sky and detect X-ray sources in the 0.1 – 10 keV energy band [39]. *Chandra* is equipped with two imaging detectors: The Advanced CCD Imaging Spectrometer (ACIS), and the High Resolution Camera (HRC).

For the purpose of this work, we use the latest release of the *Chandra* Source Catalog (CSC 2.0, CSC hereinafter) of X-ray sources [40, 41]. The catalog provides

observed properties in multiple energy bands for about 320000 compact and extended X-ray sources, as well as details of stacked-observation and detection regions.

Among the CSC data products, multi-band limiting sensitivity maps are available. We focus on a region of interest (ROI) of $6^\circ \times 6^\circ$ about the Galactic center, and retrieve sensitivity maps from the *Chandra* data base <https://cxc.harvard.edu/csc/columns/limsens.html>, binned with a 1×1 arcmin² pixel size in (l, b) . Our baseline sensitivity map corresponds to the estimated minimum energy flux in the ACIS broad band (B , 0.5 – 7.0 keV) for a source to be detected and classified as TRUE or MARGINAL at the detection position. The choice of the detection likelihood class only mildly impacts the selection of CSC sources (see App. C).

Averaging over 100 Monte Carlo simulations of the Galactic MSP population, we find 14010 ± 91 MSPs in the chosen ROI, as displayed by the orange histogram in Fig. 2. We compute the number of “detectable” MSPs that have absorbed energy flux larger than the *Chandra* sensitivity at the source position. While the number of foreground MSPs from the disk is negligible (1 ± 1 detectable MSPs), we obtain 60 ± 7 MSPs detectable from the BB, and 34 ± 6 from the NB, adding up to a total of 95 ± 9 detectable MSPs. The energy flux distributions of the Galactic MSPs population and its bulge components are shown in Fig. 2. Between vertical dotted lines in Fig. 2, we also highlight the most credible interval of our model, where the γ -to-X connection is directly supported by data: The left and right dotted lines are the fluxes that correspond to the minimal and maximal luminosity of observed X-ray MSPs, respectively, if we were to project those sources at the Galactic center.

For a meaningful comparison between Monte Carlo and *Chandra* catalogs, from the CSC we select non-variable compact sources whose energy flux in the ACIS wide band, i.e. `flux_aper90_b`, is larger than the limiting sensitivity at the source position. With these minimal cuts we select 6918 sources in our ROI, including 6837 sources having at least one intra-wide-band flux information provided. Hence, detectable MSP sources represent 1.4% of the full *Chandra* catalog in the ROI of interest. However, we show below that this fraction can be significantly enhanced with appropriate spectral and distance cuts.

Spectral observables. In order to exploit the X-ray spectral information and reject *Chandra* candidates unsuitable to be MSPs, we define the *flux ratios*:

$$\phi_{ij} = \frac{F_i - F_j}{F_i + F_j}, \quad (2)$$

where F_i is the absorbed energy flux in the i band (`flux_aper90_i` in the CSC): Hard (H , 2 – 7 keV), medium (M , 1.2 – 2 keV), and soft (S , 0.5 – 1.2 keV). We also introduce the *band fractions*:

$$\beta_i = \frac{F_i}{F_B}, \quad (3)$$

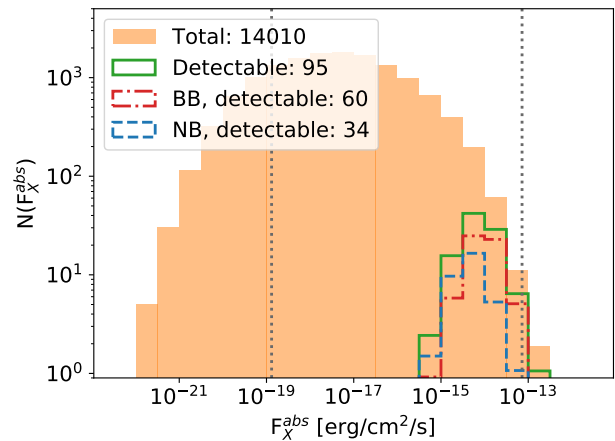


FIG. 2. X-ray energy flux distribution (0.5 – 7 keV) of the synthetic MSP population, averaged over 100 Monte Carlo simulations: Total MSPs in the ROI of interest (orange filled), total detectable MSPs (green solid) including MSPs from BB (red dot-dashed), NB (blue dashed) and disk (not shown). The vertical dotted lines illustrate the validity range of our model extrapolation (see text for details).

where i refers to the H , M or S bands defined above, and B is the ACIS broad band. From the simulated (absorbed) energy fluxes, we calculate these quantities for the detectable bulge MSP population. From over 100 Monte Carlo simulations, the extreme ranges of MSP spectral observables are: $-0.066 < \phi_{HM} < 1$, $-0.015 < \phi_{HS} < 1$, and $0.051 < \phi_{MS} < 1$, and $0.32 < \beta_H < 1$, $0.00015 < \beta_M < 0.44$ and $0 < \beta_S < 0.33$.

Optical astrometry with Gaia. The *Gaia* ESA mission [42] provides μ -arcsec astrometry for more than 1 billion stars down to magnitudes of about 20 in the white-light G band (330–1050 nm), complemented by radial-velocity and photometric information. The latest *Gaia* data release DR2 [43] contains positions and G band magnitudes for 1.7 billion sources. Among them, about 1.3 billion sources possess parallaxes. For those, distances have been determined using a probabilistic approach, and a self-consistent, reduced, catalog has been compiled [44]. In what follows, we make use of this *Gaia* catalog if not stated otherwise.

A recent study of optical counterparts of pulsars in the ATNF catalogue [45] has revealed that only 18 MSPs, in binary systems, out of 107 MSP show an optical *Gaia* counterpart. This sample is mostly local, indicating that MSP companions are typically rather dim with apparent magnitude between 18 – 20 at distances of 1 – 2 kpc. While MSPs in the Galactic disk may therefore possess optical *Gaia* counterparts, MSPs in the bulge, at 4 – 10 times higher distances, should be invisible for *Gaia*. We use the presence of optical counterparts and distance information to further reduce our sample of sought-after bulge MSP candidates, knowing that the bulge size covers $5.24 \text{ kpc} < d < 11.98 \text{ kpc}$ as extracted from our

Monte Carlo simulations. We define a positive cross-match whenever a *Gaia* source is found within the 95% C.L. semi-major axis of the error ellipse of a CSC source, `err_ellipse_r0`. Out of the 6918 sources of our initial catalog, we find 1963 *Chandra-Gaia* positive cross-matches.

We make use of spectral observables and *Gaia* astrometry to further reduce the sample of CSC sources of interest. We define two different selections.

Conservative selection. This selection of CSC sources is meant to reject most of the *Chandra* sources that we can safely say are *not compatible* with spectral and distance distributions of detectable bulge MSPs. To the 6918 non-variable, non-extended sources above the sensitivity threshold in our *Chandra* ROI, we impose that: i) Whenever a spectral observable is available, the source is retained only if its value falls within the corresponding Monte Carlo-deduced range. If intra-wide-band fluxes are zero or unavailable (as typically occurs for too dim sources), the source is *kept*. This reduces the sample to 3606 objects. ii) If the distances of all *Gaia* counterparts are either closer than the distance to the bulge or further away, i.e. the source is in the disk, the source is *rejected*. This further reduces the selected sources down to 2981. For illustration, by reducing the cross-matching radius to 1 arcsec (of the order of the systematic error on the positional reconstruction), we get 1047 cross-matches between the 6918 *Chandra* and *Gaia* catalogs, ending up with 3192 sources in our conservative selection.

Aggressive selection. This second selection aims at isolating the *most promising* sample of bulge “MSP-like” candidates. To this end, we keep sources: i) For which all ϕ_{ij} ’s and β_i ’s are computable and fall within our Monte Carlo extreme intervals. This reduces the sample to 589 objects. ii) That have *no cross-matches* with *Gaia* sources, following the rationale discussed above. By doing so, we discard sources that are surely in the disk (221), sources that may be in the disk or in the bulge (21), and, finally, also sources that are surely in the bulge (52). This reduces the sample to only 295 objects. Such a selection is not based on *Gaia* distance information, and therefore the full *Gaia* DR2 catalog [43] can also be used. In this case, the aggressive sample would reduce to 232 candidates.

We display the energy flux distribution of our two selected samples and of our detectable Monte Carlo sample in Fig. 3. By comparing the flux distributions of our synthetic MSP population and of CSC selected candidates, we can see that *the bulge MSP model is consistent with current X-ray observations*. The aggressive source selection provides a sub-sample of *Chandra* objects which is suitable for further investigation, as discussed in the next section. Further improvements in the selection of MSP-like candidates can be achieved by cuts on the flux interval. Our conclusions hold true against some systematic uncertainties, such as the GLF of bulge MSPs and modeling of the X-ray absorption (see App. B).

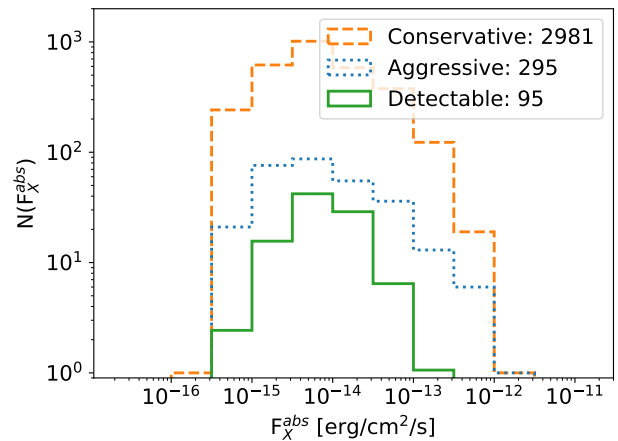


FIG. 3. As in Fig. 2, showing Monte Carlo predictions for the total number of detectable MSPs (green solid), together with the conservative CSC selection (orange dashed) and the aggressive (blue dotted) CSC selection.

Finally, potentially constraining information is encoded in the spatial distribution of sources. This can be exploited to optimize the ROI by maximizing the ratio of detectable-to-candidate sources, see App. D for an illustration. However, such a procedure would strongly rely on the assumption that the MSP spatial modeling is valid down to small scales, while we know that the γ -ray observations on which it is based on are much more coarse grained. Therefore, we decide not to pursue our analysis further in this direction.

Prospects and conclusions. We have shown *for the first time* that a simple model for a population of MSPs in the Galactic bulge, which can account for the excess γ -ray emission seen by the *Fermi-LAT*, i) is consistent with current X-ray *Chandra* observations of compact sources and ii) together with information from *Gaia*, it allows one to select a few hundreds *Chandra* sources most promising for follow-up studies. Our work represents a first proof-of-principle of the potential of X-ray searches for bulge MSPs. Let us conclude by briefly discussing possible improvements as well as promising extensions of this analysis.

Characterizing the non-thermal multi-wavelength spectrum of a large sample of MSPs (as done, for example, in [46, 47] mostly for pulsars) would set population studies of MSP emission mechanisms on more solid grounds and improve our understanding of the γ -X connection. Dedicated analyses of archived X-ray observations and existing source catalogs is another path to refine the spectral selection of MSP candidates, distinguishing them from extragalactic objects and other Galactic sources as cataclysmic variables and intermediate polars.

A perhaps more promising extension of this study would be to engage in a multi-wavelength analysis of existing data, in particular in the radio and infrared bands,

and to design follow-up campaigns to further isolate MSP candidates in the Galactic bulge [48] (see [49, 50] for applications to globular clusters). Spectral characterization of MSPs vs. alternative sources are a pre-requisite for such studies. The sample selected with our “aggressive” cuts is the most interesting starting point for these further analyses that we plan to perform.

In conclusion, our findings open up new and exciting avenues to look for bulge MSPs and their connection with the GeV excess with X-ray observations. If supplemented with multiwavelength observations, these have the potential to provide breakthrough results in the near future.

Acknowledgments. We warmly acknowledge enlightening discussions with and comments on the draft

by L. Guillemot. We thank T. D. P. Edwards for fruitful discussions about the γ -ray luminosity function. The PhD fellowship of J. B. is supported by the Mission pour les initiatives transverses et interdisciplinaires (MITI), CNRS (SMilERX project). We acknowledge support from Agence Nationale de la Recherche AAPG2019, project GECO (PI: F.C.). M.C., G.D., and P.-O.P. acknowledge support from CNES and the *Programme National Hautes Energies* (CNRS/PNHE). This research has made use of data obtained from the Chandra Source Catalog, provided by the Chandra X-ray Center (CXC) as part of the Chandra Data Archive and of data from the European Space Agency (ESA) mission Gaia, processed by the Gaia Data Processing and Analysis Consortium (DPAC).

-
- [1] K. N. Abazajian and M. Kaplinghat, *Phys. Rev.* **D86**, 083511 (2012), [arXiv:1207.6047 \[astro-ph.HE\]](#).
- [2] C. Gordon and O. Macias, *Phys. Rev.* **D88**, 083521 (2013), [Erratum: *Phys. Rev.*D89,no.4,049901(2014)], [arXiv:1306.5725 \[astro-ph.HE\]](#).
- [3] F. Calore, I. Cholis, and C. Weniger, *Journal of Cosmology and Astroparticle Physics* **1503**, 038, [arXiv:1409.0042 \[astro-ph.CO\]](#).
- [4] T. Daylan, D. P. Finkbeiner, D. Hooper, T. Linden, S. K. N. Portillo, N. L. Rodd, and T. R. Slatyer, *Phys. Dark Univ.* **12**, 1 (2016), [arXiv:1402.6703 \[astro-ph.HE\]](#).
- [5] M. Ajello et al. (Fermi-LAT), *Astrophys. J.* **819**, 44 (2016), [arXiv:1511.02938 \[astro-ph.HE\]](#).
- [6] K. N. Abazajian, *Journal of Cosmology and Astroparticle Physics* **1103**, 010, [arXiv:1011.4275 \[astro-ph.HE\]](#).
- [7] F. Calore, I. Cholis, C. McCabe, and C. Weniger, *Phys. Rev.* **D91**, 063003 (2015), [arXiv:1411.4647 \[hep-ph\]](#).
- [8] R. Bartels, E. Storm, C. Weniger, and F. Calore, *Nature Astronomy* **2**, 819 (2018), [arXiv:1711.04778 \[astro-ph.HE\]](#).
- [9] O. Macias, C. Gordon, R. M. Crocker, B. Coleman, D. Paterson, S. Horiuchi, and M. Pohl, *Nature Astronomy* **2**, 387 (2018), [arXiv:1611.06644 \[astro-ph.HE\]](#).
- [10] R. Bartels, S. Krishnamurthy, and C. Weniger, *Phys. Rev. Lett.* **116**, 051102 (2016).
- [11] S. K. Lee, M. Lisanti, B. R. Safdi, T. R. Slatyer, and W. Xue, *Phys. Rev. Lett.* **116**, 051103 (2016).
- [12] R. K. Leane and T. R. Slatyer, *Phys. Rev. Lett.* **123**, 241101 (2019), [arXiv:1904.08430 \[astro-ph.HE\]](#).
- [13] R. K. Leane and T. R. Slatyer, *arXiv e-prints*, [arXiv:2002.12370](#) (2020), [arXiv:2002.12370 \[astro-ph.HE\]](#).
- [14] L. J. Chang, S. Mishra-Sharma, M. Lisanti, M. Buschmann, N. L. Rodd, and B. R. Safdi, *Phys. Rev. D* **101**, 023014 (2020), [arXiv:1908.10874 \[astro-ph.CO\]](#).
- [15] M. Buschmann, N. L. Rodd, B. R. Safdi, L. J. Chang, S. Mishra-Sharma, M. Lisanti, and O. Macias, *Phys. Rev. D* **102**, 023023 (2020), [arXiv:2002.12373 \[astro-ph.HE\]](#).
- [16] Y.-M. Zhong, S. D. McDermott, I. Cholis, and P. J. Fox, *Phys. Rev. Lett.* **124**, 231103 (2020), [arXiv:1911.12369 \[astro-ph.HE\]](#).
- [17] F. Calore, M. Di Mauro, F. Donato, J. W. T. Hessels, and C. Weniger, *Astrophys. J.* **827**, 143 (2016), [arXiv:1512.06825 \[astro-ph.HE\]](#).
- [18] F. Calore, T. Regimbau, and P. D. Serpico, *Phys. Rev. Lett.* **122**, 081103 (2019), [arXiv:1812.05094 \[astro-ph.HE\]](#).
- [19] S. Bogdanov, in *Pulsar Astrophysics the Next Fifty Years*, IAU Symposium, Vol. 337, edited by P. Weltevrede, B. B. P. Perera, L. L. Preston, and S. Sanidas (2018) pp. 116–119, [arXiv:1711.04791 \[astro-ph.HE\]](#).
- [20] M. Marelli, A. De Luca, and P. A. Caraveo, *Astrophys. J.* **733**, 82 (2011), [arXiv:1103.0572 \[astro-ph.HE\]](#).
- [21] M. Marelli, R. Mignani, A. De Luca, P. Saz Parkinson, D. Salvetti, P. Den Hartog, and M. Wolff, *Astrophys. J.* **802**, 78 (2015), [arXiv:1501.06215 \[astro-ph.HE\]](#).
- [22] J. Lee, C. Y. Hui, J. Takata, A. K. H. Kong, P. H. T. Tam, and K. S. Cheng, *Astrophys. J.* **864**, 23 (2018), [arXiv:1807.06505 \[astro-ph.HE\]](#).
- [23] R. T. Bartels, T. D. P. Edwards, and C. Weniger, *Monthly Notices of the Royal Astronomical Society* **481**, 3966 (2018), [arXiv:1805.11097 \[astro-ph.HE\]](#).
- [24] R. Bartels, D. Hooper, T. Linden, S. Mishra-Sharma, N. L. Rodd, B. R. Safdi, and T. R. Slatyer, *Phys. Dark Univ.* **20**, 88 (2018), [arXiv:1710.10266 \[astro-ph.HE\]](#).
- [25] L. Cao, S. Mao, D. Nataf, N. J. Rattenbury, and A. Gould, *Monthly Notices of the Royal Astronomical Society* **434**, 595 (2013), [arXiv:1303.6430 \[astro-ph.GA\]](#).
- [26] R. Launhardt, R. Zylka, and P. G. Mezger, *Astronomy and Astrophysics* **384**, 112 (2002), [arXiv:astro-ph/0201294 \[astro-ph\]](#).
- [27] H. Ploeg, C. Gordon, R. Crocker, and O. Macias, *Journal of Cosmology and Astroparticle Physics* **1708** (08), 015, [arXiv:1705.00806 \[astro-ph.HE\]](#).
- [28] H. Ploeg, C. Gordon, R. Crocker, and O. Macias, *arXiv e-prints*, [arXiv:2008.10821](#) (2020), [arXiv:2008.10821 \[astro-ph.HE\]](#).
- [29] A. Possenti, R. Cerutti, M. Colpi, and S. Mereghetti, *Astronomy & Astrophysics* **387**, 993 (2002), [arXiv:astro-ph/0109452 \[astro-ph\]](#).
- [30] C. Kalapotharakos, A. K. Harding, D. Kazanas, and Z. Wadiasingh, *Astrophys. J. Letters* **883**, L4 (2019), [arXiv:1904.01765 \[astro-ph.HE\]](#).
- [31] D.-H. Wang, C.-M. Zhang, and S.-Q. Wang, *Publications of the Astronomical Society of the Pacific* **131**, 024201 (2019), [arXiv:1910.08317 \[astro-ph.HE\]](#).

- [32] S. Abdollahi, F. Acero, M. Ackermann, M. Ajello, W. B. Atwood, M. Axelsson, L. Baldini, J. Ballet, G. Barbiellini, D. Bastieri, J. Becerra Gonzalez, R. Bellazzini, A. Berretta, E. Bissaldi, R. D. Blandford, E. D. Bloom, R. Bonino, E. Bottacini, T. J. Brandt, J. Bregeon, P. Bruel, R. Buehler, T. H. Burnett, S. Buson, R. A. Cameron, R. Caputo, P. A. Caraveo, J. M. Casandjian, D. Castro, E. Cavazzuti, E. Charles, S. Chaty, S. Chen, C. C. Cheung, G. Chiaro, S. Ciprini, J. Cohen-Tanugi, L. R. Cominsky, J. Coronado-Blázquez, D. Costantin, A. Cuoco, S. Cutini, F. D’Ammando, M. DeKlotz, P. d. I. Torre Luque, F. de Palma, A. Desai, S. W. Digel, N. D. Lalla, M. D. Mauro, L. D. Venere, A. Domínguez, D. Dumora, F. F. Dirrsa, S. J. Fegan, E. C. Ferrara, A. Franckowiak, Y. Fukazawa, S. Funk, P. Fusco, F. Gargano, D. Gasparrini, N. Giglietto, P. Giommi, F. Giordano, M. Giroletti, T. Glanzman, D. Green, I. A. Grenier, S. Grifflin, M. H. Grondin, J. E. Grove, S. Guiriec, A. K. Harding, K. Hayashi, E. Hays, J. W. Hewitt, D. Horan, G. Jóhannesson, T. J. Johnson, T. Kamae, M. Kerr, D. Kocevski, M. Kovac’evic’, M. Kuss, D. Landriu, S. Larsson, L. Latronico, M. Lemoine-Goumard, J. Li, I. Liodakis, F. Longo, F. Loparco, B. Lott, M. N. Lovellette, P. Lubrano, G. M. Madejski, S. Maldera, D. Malyshev, A. Manfreda, E. J. Marchesini, L. Marcotulli, G. Martí-Devesa, P. Martin, F. Massaro, M. N. Mazziotta, J. E. McEnery, I. Mereu, M. Meyer, P. F. Michelson, N. Mirabal, T. Mizuno, M. E. Monzani, A. Morselli, I. V. Moskalenko, M. Negro, E. Nuss, R. Ojha, N. Omodei, M. Orienti, E. Orlando, J. F. Ormes, M. Palatiello, V. S. Paliya, D. Paneque, Z. Pei, H. Peña-Herazo, J. S. Perkins, M. Persic, M. Pesce-Rollins, V. Petrosian, L. Petrov, F. Piron, H. Poon, T. A. Porter, G. Principe, S. Rainò, R. Rando, M. Razzano, S. Razzaque, A. Reimer, O. Reimer, Q. Remy, T. Reposeur, R. W. Romani, P. M. S. Parkinson, F. K. Schinzel, D. Serini, C. Sgrò, E. J. Siskind, D. A. Smith, G. Spandre, P. Spinelli, A. W. Strong, D. J. Suson, H. Tajima, M. N. Takahashi, D. Tak, J. B. Thayer, D. J. Thompson, L. Tibaldo, D. F. Torres, E. Torresi, J. Valverde, B. V. Klaveren, P. v. Zyl, K. Wood, M. Yassin, and G. Zaharijas, *Astrophys. J. Supplement Series* **247**, 33 (2020), [arXiv:1902.10045 \[astro-ph.HE\]](#).
- [33] F. Pedregosa, G. Varoquaux, A. Gramfort, V. Michel, B. Thirion, O. Grisel, M. Blondel, P. Prettenhofer, R. Weiss, V. Dubourg, J. Vanderplas, A. Passos, D. Cournapeau, M. Brucher, M. Perrot, and E. Duchesnay, *Journal of Machine Learning Research* **12**, 2825 (2011).
- [34] M. Balucinska-Church and D. McCammon, *Astrophys. J.* **400**, 699 (1992).
- [35] E. Anders and N. Grevesse, *Geochimica et Cosmochimica Acta* **53**, 197 (1989).
- [36] P. M. W. Kalberla, W. B. Burton, D. Hartmann, E. M. Arnal, E. Bajaja, R. Morras, and W. G. L. Pöppel, *Astronomy & Astrophysics* **440**, 775 (2005), [arXiv:astro-ph/0504140 \[astro-ph\]](#).
- [37] T. Dame, D. Hartmann, and P. Thaddeus, *Astrophys. J.* **547**, 792 (2001), [arXiv:astro-ph/0009217](#).
- [38] I. A. Grenier, J.-M. Casandjian, and R. Terrier, *Science* **307**, 1292 (2005).
- [39] M. Weisskopf, B. Brinkman, C. Canizares, G. Garmire, S. Murray, and L. Van Speybroeck, *The Publications of the Astronomical Society of the Pacific* **114**, 1 (2002), [arXiv:astro-ph/0110308](#).
- [40] I. N. Evans, F. A. Primini, K. J. Glotfelty, C. S. Anderson, N. R. Bonaventura, J. C. Chen, J. E. Davis, S. M. Doe, J. D. Evans, G. Fabbiano, E. C. Galle, I. Gibbs, Danny G., J. D. Grier, R. M. Hain, D. M. Hall, P. N. Harbo, X. H. He, J. C. Houck, M. Karovska, V. L. Kashyap, J. Lauer, M. L. McCollough, J. C. McDowell, J. B. Miller, A. W. Mitschang, D. L. Morgan, A. E. Mossman, J. S. Nichols, M. A. Nowak, D. A. Plummer, B. L. Refsdal, A. H. Rots, A. Siemiginowska, B. A. Sundheim, M. S. Tibbetts, D. W. Van Stone, S. L. Winkelman, and P. Zografou, *Astrophys. J. Supplement* **189**, 37 (2010), [arXiv:1005.4665 \[astro-ph.HE\]](#).
- [41] F. A. Primini, C. E. Allen, J. Miller, C. S. Anderson, J. A. Budynkiewicz, D. Burke, J. C. Chen, F. M. Civano, R. D’Abrusco, S. M. Doe, I. N. Evans, J. D. Evans, G. Fabbiano, I. Gibbs, Danny G., K. J. Glotfelty, D. E. Graessle, J. D. Grier, R. Hain, D. M. Hall, P. N. Harbo, J. C. Houck, J. L. Lauer, O. Laurino, N. P. Lee, J. R. Martínez-Galarza, M. L. McCollough, J. C. McDowell, W. McLaughlin, D. L. Morgan, A. E. Mossman, D. T. Nguyen, J. S. Nichols, M. A. Nowak, C. Paxson, D. A. Plummer, A. H. Rots, A. Siemiginowska, B. A. Sundheim, M. Tibbetts, D. W. Van Stone, and P. Zografou, in *American Astronomical Society Meeting Abstracts #231*, American Astronomical Society Meeting Abstracts, Vol. 231 (2018) p. 238.02.
- [42] Gaia Collaboration, T. Prusti, J. H. J. de Bruijne, A. G. A. Brown, A. Vallenari, C. Babusiaux, C. A. L. Bailer-Jones, U. Bastian, M. Biermann, D. W. Evans, L. Eyer, F. Jansen, C. Jordi, S. A. Klioner, U. Lammers, L. Lindgren, X. Luri, F. Mignard, D. J. Milligan, C. Panem, V. Poinsignon, D. Pourbaix, S. Randich, G. Sarri, P. Sartoretti, H. I. Siddiqui, C. Soubiran, V. Valette, F. van Leeuwen, N. A. Walton, C. Aerts, F. Arenou, M. Cropper, R. Drimmel, E. Høg, D. Katz, M. G. Lattanzi, W. O’Mullane, E. K. Grebel, A. D. Holland, C. Huc, X. Passot, L. Bramante, C. Cacciari, J. Castañeda, L. Chaoul, N. Cheek, F. De Angeli, C. Fabricius, R. Guerra, J. Hernández, A. Jean-Antoine-Piccolo, E. Masana, R. Messineo, N. Mowlavi, K. Nienartowicz, D. Ordóñez-Blanco, P. Panuzzo, J. Portell, P. J. Richards, M. Riello, G. M. Seabroke, P. Tanga, F. Thévenin, J. Torra, S. G. Els, G. Gracia-Abril, G. Comoretto, M. Garcia-Reinaldos, T. Lock, E. Mercier, M. Altmann, R. Andrae, T. L. Astraatmadja, I. Bellas-Velidis, K. Benson, J. Berthier, R. Blomme, G. Busso, B. Carry, A. Cellino, G. Clementini, S. Cowell, O. Creevey, J. Cuypers, M. Davidson, J. De Ridder, A. de Torres, L. Delchambre, A. Dell’Oro, C. Ducourant, Y. Frémat, M. García-Torres, E. Gosset, J. L. Halbwachs, N. C. Hambly, D. L. Harrison, M. Hauser, D. Hestroffer, S. T. Hodgkin, H. E. Huckle, A. Hutton, G. Jasiewicz, S. Jordan, M. Kontizas, A. J. Korn, A. C. Lanzafame, M. Manteiga, A. Moitinho, K. Muinonen, J. Osinde, E. Pancino, T. Pauwels, J. M. Petit, A. Recio-Blanco, A. C. Robin, L. M. Sarro, C. Siopis, M. Smith, K. W. Smith, A. Sozzetti, W. Thuillot, W. van Reeve, Y. Viala, U. Abbas, A. Abreu Aramburu, S. Accart, J. J. Aguado, P. M. Allan, W. Allasia, G. Altavilla, M. A. Álvarez, J. Alves, R. I. Anderson, A. H. Andrei, E. Anglada Varela, E. Antiche, T. Antoja, S. Antón, B. Arcay, A. Atzei, L. Ayache, N. Bach, S. G. Baker, L. Balaguer-Núñez, C. Barache, C. Barata, A. Barbier, F. Barblan, M. Baroni, D. Barrado y Navascués,

- M. Barros, M. A. Barstow, U. Becciani, M. Bellazzini, G. Bellei, A. Bello García, V. Belokurov, P. Bendjoya, A. Berihuete, L. Bianchi, O. Bienaymé, F. Billebaud, N. Blagorodnova, S. Blanco-Cuaresma, T. Boch, A. Bombrun, R. Borrachero, S. Bouquillon, G. Bourda, H. Bouy, A. Bragaglia, M. A. Breddels, N. Brouillet, T. Brüsemeister, B. Bucciarelli, F. Budnik, P. Burgess, R. Burgon, A. Burlacu, D. Busonero, R. Buzzi, E. Caffau, J. Cambras, H. Campbell, R. Cancelliere, T. Cantat-Gaudin, T. Carlucci, J. M. Carrasco, M. Castellani, P. Charlot, J. Charnas, P. Charvet, F. Chassat, A. Chivassa, M. Clotet, G. Coccozza, R. S. Collins, P. Collins, G. Costigan, F. Crifo, N. J. G. Cross, M. Crosta, C. Crowley, C. Dafonte, Y. Damerджи, A. Dapergolas, P. David, M. David, P. De Cat, F. de Felice, P. de Laverny, F. De Luise, R. De March, D. de Martino, R. de Souza, J. Debosscher, E. del Pozo, M. Delbo, A. Delgado, H. E. Delgado, F. di Marco, P. Di Matteo, S. Diakite, E. Distefano, C. Dolding, S. Dos Anjos, P. Drazinos, J. Durán, Y. Dzigan, E. Ecale, B. Edvardsson, H. Enke, M. Erdmann, D. Escolar, M. Espina, N. W. Evans, G. Eynard Bontemps, C. Fabre, M. Fabrizio, S. Faigler, A. J. Falcão, M. Farràs Casas, F. Faye, L. Federici, G. Fedorets, J. Fernández-Hernández, P. Fernique, A. Fienga, F. Figueras, F. Filippi, K. Findeisen, A. Fonti, M. Fouesneau, E. Fraile, M. Fraser, J. Fuchs, R. Furnell, M. Gai, S. Galleti, L. Galluccio, D. Garabato, F. García-Sedano, P. Garé, A. Garofalo, N. Garralda, P. Gavras, J. Gerssen, R. Geyer, G. Gilmore, S. Girona, G. Giuffrida, M. Gomes, A. González-Marcos, J. González-Núñez, J. J. González-Vidal, M. Granvik, A. Guerrier, P. Guillout, J. Guiraud, A. Gúrpide, R. Gutiérrez-Sánchez, L. P. Guy, R. Haigron, D. Hatzidimitriou, M. Haywood, U. Heiter, A. Helmi, D. Hobbs, W. Hoffmann, B. Holl, G. Holland, J. A. S. Hunt, A. Hypki, V. Icardi, M. Irwin, G. Jevardat de Fombelle, P. Jofré, P. G. Jonker, A. Jorissen, F. Julbe, A. Karampelas, A. Kochoska, R. Kohley, K. Kolenberg, E. Kontizas, S. E. Koposov, G. Kordopatis, P. Koubsky, A. Kowalczyk, A. Krone-Martins, M. Kudryashova, I. Kull, R. K. Bachchan, F. Lacoste-Seris, A. F. Lanza, J. B. Lavigne, C. Le Poncin-Lafitte, Y. Lebreton, T. Lebzelter, S. Leccia, N. Leclerc, I. Lecoeur-Taibi, V. Lemaitre, H. Lenhardt, F. Leroux, S. Liao, E. Licata, H. E. P. Lindstrøm, T. A. Lister, E. Livanou, A. Lobel, W. Löffler, M. López, A. Lopez-Lozano, D. Lorenz, T. Loureiro, I. MacDonald, T. Magalhães Fernandes, S. Managau, R. G. Mann, G. Mantelet, O. Marchal, J. M. Marchant, M. Marconi, J. Marie, S. Marinoni, P. M. Marrese, G. Marschalkó, D. J. Marshall, J. M. Martín-Fleitas, M. Martino, N. Mary, G. Matijević, T. Mazeh, P. J. McMillan, S. Messina, A. Mestre, D. Michalik, N. R. Millar, B. M. H. Miranda, D. Molina, R. Molinaro, M. Molinaro, L. Molnár, M. Moniez, P. Montegriffo, D. Monteiro, R. Mor, A. Mora, R. Morbidelli, T. Morel, S. Morgenthaler, T. Morley, D. Morris, A. F. Mulone, T. Muraveva, I. Musella, J. Narbonne, G. Nelemans, L. Nicastro, L. Noval, C. Ordénovic, J. Ordieres-Meré, P. Osborne, C. Pagani, I. Pagano, F. Pailler, H. Palacin, L. Palaversa, P. Parsons, T. Paulsen, M. Pecoraro, R. Pedrosa, H. Pentikäinen, J. Pereira, B. Pichon, A. M. Pierimoni, F. X. Pineau, E. Plachy, G. Plum, E. Poujoulet, A. Prša, L. Pulone, S. Ragaini, S. Rago, N. Rambaux, M. Ramos-Lerate, P. Ranalli, G. Rauw, A. Read, S. Regibo, F. Renk, C. Reylé, R. A. Ribeiro, L. Rimoldini, V. Ripepi, A. Riva, G. Rixon, M. Roelens, M. Romero-Gómez, N. Rowell, F. Royer, A. Rudolph, L. Ruiz-Dern, G. Sadowski, T. Sagristà Sellés, J. Sahlmann, J. Salgado, E. Salguero, M. Sarasso, H. Savietto, A. Schnorhk, M. Schultheis, E. Sciacca, M. Segol, J. C. Segovia, D. Segransan, E. Serpell, I. C. Shih, R. Smareglia, R. L. Smart, C. Smith, E. Solano, F. Solitro, R. Sordo, S. Soria Nieto, J. Souchay, A. Spagna, F. Spoto, U. Stampa, I. A. Steele, H. Steidelmüller, C. A. Stephenson, H. Stoev, F. F. Suess, M. Süveges, J. Surdej, L. Szabados, E. Szegedi-Elek, D. Tapiador, F. Taris, G. Tauran, M. B. Taylor, R. Teixeira, D. Terrett, B. Tingley, S. C. Trager, C. Turon, A. Ulla, E. Utrilla, G. Valentini, A. van Elteren, E. Van Hemelryck, M. van Leeuwen, M. Varadi, A. Vecchiato, J. Veljanoski, T. Via, D. Vicente, S. Vogt, H. Voss, V. Votruba, S. Voutsinas, G. Walmsley, M. Weiler, K. Weingrill, D. Werner, T. Wevers, G. Whitehead, L. Wyrzykowski, A. Yoldas, M. Žerjal, S. Zucker, C. Zurbach, T. Zwitter, A. Alecu, M. Allen, C. Allende Prieto, A. Amorim, G. Anglada-Escudé, V. Arsenijevic, S. Azaz, P. Balm, M. Beck, H. H. Bernstein, L. Bigot, A. Bijaoui, C. Blasco, M. Bonfigli, G. Bono, S. Boudreault, A. Bressan, S. Brown, P. M. Brunet, P. Bunclark, R. Buonanno, A. G. Butkevich, C. Carret, C. Carion, L. Chemin, F. Chéreau, L. Corcione, E. Darmigny, K. S. de Boer, P. de Teodoro, P. T. de Zeeuw, C. Delle Luche, C. D. Domingues, P. Dubath, F. Fodor, B. Frézouls, A. Fries, D. Fustes, D. Fyfe, E. Gallardo, J. Gallejos, D. Gardiol, M. Gebran, A. Gomboc, A. Gómez, E. Grux, A. Gueguen, A. Heyrovsky, J. Hoar, G. Iannicola, Y. Isasi Parache, A. M. Janotto, E. Joliet, A. Jonckheere, R. Keil, D. W. Kim, P. Klagyivik, J. Klar, J. Knude, O. Kochukhov, I. Kolka, J. Kos, A. Kutka, V. Lainey, D. LeBouquin, C. Liu, D. Loreggia, V. V. Makarov, M. G. Marseille, C. Martayan, O. Martinez-Rubi, B. Massart, F. Meynadier, S. Mignot, U. Munari, A. T. Nguyen, T. Nordlander, P. Ocvirk, K. S. O’Flaherty, A. Olias Sanz, P. Ortiz, J. Osorio, D. Ozkiewicz, A. Ouzounis, M. Palmer, P. Park, E. Pasquato, C. Peltzer, J. Peralta, F. Péturaud, T. Pieniluoma, E. Pigozzi, J. Poels, G. Prat, T. Prod’homme, F. Raison, J. M. Rebordao, D. Risquez, B. Rocca-Volmerange, S. Rosen, M. I. Ruiz-Fuertes, F. Russo, S. Sembay, I. Serraller Vizcaino, and A. Short, .
- [43] Gaia Collaboration, A. G. A. Brown, A. Vallenari, T. Prusti, J. H. J. de Bruijne, C. Babusiaux, C. A. L. Bailer-Jones, M. Biermann, D. W. Evans, L. Eyer, F. Jansen, C. Jordi, S. A. Klioner, U. Lammers, L. Lindgren, X. Luri, F. Mignard, C. Panem, D. Pourbaix, S. Randich, P. Sartoretti, H. I. Siddiqui, C. Soubiran, F. van Leeuwen, N. A. Walton, F. Arenou, U. Bastian, M. Cropper, R. Drimmel, D. Katz, M. G. Lattanzi, J. Bakker, C. Cacciari, J. Castañeda, L. Chaoul, N. Cheek, F. De Angeli, C. Fabricius, R. Guerra, B. Holl, E. Masana, R. Messineo, N. Mowlavi, K. Nienartowicz, P. Panuzzo, J. Portell, M. Riello, G. M. Seabroke, P. Tanga, F. Thévenin, G. Gracia-Abril, G. Comoretto, M. Garcia-Reinaldos, D. Teyssier, M. Altmann, R. Andrae, M. Audard, I. Bellas-Velidis, K. Benson, J. Berthier, R. Blomme, P. Burgess, G. Busso, B. Carry, A. Cellino, G. Clementini, M. Clotet, O. Creevey, M. Davidson, J. De Ridder, L. Delchambre, A. Dell’Oro, C. Ducourant, J. Fernández-Hernández, M. Fouesneau,

- Y. Frémat, L. Galluccio, M. García-Torres, J. González-Núñez, J. J. González-Vidal, E. Gosset, L. P. Guy, J. L. Halbwachs, N. C. Hambly, D. L. Harrison, J. Hernández, D. Hestroffer, S. T. Hodgkin, A. Hutton, G. Jasiewicz, A. Jean-Antoine-Piccolo, S. Jordan, A. J. Korn, A. Krone-Martins, A. C. Lanzafame, T. Lebzelter, W. Löffler, M. Manteiga, P. M. Marrese, J. M. Martín-Fleitas, A. Moitinho, A. Mora, K. Muinonen, J. Osinde, E. Pancino, T. Pauwels, J. M. Petit, A. Recio-Blanco, P. J. Richards, L. Rimoldini, A. C. Robin, L. M. Sarro, C. Siopis, M. Smith, A. Sozzetti, M. Süveges, J. Torra, W. van Reeve, U. Abbas, A. Abreu Aramburu, S. Accart, C. Aerts, G. Altavilla, M. A. Álvarez, R. Alvarez, J. Alves, R. I. Anderson, A. H. Andrei, E. Anglada Varela, E. Antiche, T. Antoja, B. Arcay, T. L. Asstraatmadja, N. Bach, S. G. Baker, L. Balaguer-Núñez, P. Balm, C. Barache, C. Barata, D. Barbato, F. Barblan, P. S. Barklem, D. Barrado, M. Barros, M. A. Barstow, S. Bartholomé Muñoz, J. L. Bassilana, U. Beciani, M. Bellazzini, A. Berihuete, S. Bertone, L. Bianchi, O. Bienaymé, S. Blanco-Cuaresma, T. Boch, C. Boeche, A. Bombrun, R. Borrachero, D. Bossini, S. Bouquillon, G. Bourda, A. Bragaglia, L. Bramante, M. A. Breddels, A. Bressan, N. Brouillet, T. Brüsemeister, E. Brugaletta, B. Bucciarelli, A. Burlacu, D. Busonero, A. G. Butkevich, R. Buzzì, E. Caffau, R. Cancelliere, G. Cannizzaro, T. Cantat-Gaudin, R. Carballo, T. Carlucci, J. M. Carrasco, L. Casamiquela, M. Castellani, A. Castro-Ginard, P. Charlot, L. Chemin, A. Chiavassa, G. Cocozza, G. Costigan, S. Cowell, F. Crifo, M. Crosta, C. Crowley, J. Cuypers, C. Dafonte, Y. Damerджи, A. Dapergolas, P. David, M. David, P. de Laverny, F. De Luise, R. De March, D. de Martino, R. de Souza, A. de Torres, J. Debosscher, E. del Pozo, M. Delbo, A. Delgado, H. E. Delgado, P. Di Matteo, S. Diakite, C. Diener, E. Distefano, C. Dolding, P. Drazinos, J. Durán, B. Edvardsson, H. Enke, K. Eriksson, P. Esquej, G. Eynard Bontemps, C. Fabre, M. Fabrizio, S. Faigler, A. J. Falcão, M. Farràs Casas, L. Federici, G. Fedorets, P. Fernique, F. Figueras, F. Filippi, K. Findeisen, A. Fonti, E. Fraile, M. Fraser, B. Frézouls, M. Gai, S. Galleti, D. Garabato, F. García-Sedano, A. Garofalo, N. Garralda, A. Gavel, P. Gavras, J. Gerssen, R. Geyer, P. Giacobbe, G. Gilmore, S. Girona, G. Giuffrida, F. Glass, M. Gomes, M. Granvik, A. Gueguen, A. Guerrier, J. Guiraud, R. Gutiérrez-Sánchez, R. Haignon, D. Hatzidimitriou, M. Hauser, M. Haywood, U. Heiter, A. Helmi, J. Heu, T. Hilger, D. Hobbs, W. Hofmann, G. Holland, H. E. Huckle, A. Hypki, V. Icardi, K. Janßen, G. Jevardat de Fombelle, P. G. Jonker, Á. L. Juhász, F. Julbe, A. Karamelas, A. Kewley, J. Klar, A. Kochoska, R. Kohley, K. Kolenberg, M. Kontizas, E. Kontizas, S. E. Koposov, G. Kordopatis, Z. Kostrzewa-Rutkowska, P. Koubsky, S. Lambert, A. F. Lanza, Y. Lasne, J. B. Lavigne, Y. Le Fustec, C. Le Poncin-Lafitte, Y. Lebreton, S. Leccia, N. Leclerc, I. Lecoœur-Taibi, H. Lenhardt, F. Leroux, S. Liao, E. Licata, H. E. P. Lindstrøm, T. A. Lister, E. Livanou, A. Lobel, M. López, S. Managau, R. G. Mann, G. Mantelet, O. Marchal, J. M. Marchant, M. Marconi, S. Marinoni, G. Marschalkó, D. J. Marshall, M. Martino, G. Marton, N. Mary, D. Massari, G. Matijević, T. Mazeh, P. J. McMillan, S. Messina, D. Michalik, N. R. Millar, D. Molina, R. Molinaro, L. Molnár, P. Montegriffo, R. Mor, R. Morbidelli, T. Morel, D. Morris, A. F. Mulone, T. Muraveva, I. Musella, G. Nelemans, L. Nicasastro, L. Noval, W. O'Mullane, C. Ordénovic, D. Ordóñez-Blanco, P. Osborne, C. Pagani, I. Pagano, F. Pailler, H. Palacin, L. Palaversa, A. Panahi, M. Pawlak, A. M. Piersimoni, F. X. Pineau, E. Plachy, G. Plum, E. Poggio, E. Poujoulet, A. Prša, L. Pulone, E. Racero, S. Ragaini, N. Rambaux, M. Ramos-Lerate, S. Regibo, C. Reylé, F. Riclet, V. Ripepi, A. Riva, A. Rivo, Rivard, G. Rixon, T. Roegiers, M. Roelens, M. Romero-Gómez, N. Rowell, F. Royer, L. Ruiz-Dern, G. Sadowski, T. Sagristà Sellés, J. Sahlmann, J. Salgado, E. Salguero, N. Sanna, T. Santana-Ros, M. Sarasso, H. Saviotto, M. Schultheis, E. Sciacca, M. Segol, J. C. Segovia, D. Ségransan, I. C. Shih, L. Siltala, A. F. Silva, R. L. Smart, K. W. Smith, E. Solano, F. Solitro, R. Sordo, S. Soria Nieto, J. Souchay, A. Spagna, F. Spoto, U. Stampa, I. A. Steele, H. Steidelmüller, C. A. Stephenson, H. Stoev, F. F. Suess, J. Surdej, L. Szabados, E. Szegedi-Elek, D. Tapiador, F. Taris, G. Tauran, M. B. Taylor, R. Teixeira, D. Terrett, P. Teyssandier, W. Thuillot, A. Titarenko, F. Torra Clotet, C. Turon, A. Ulla, E. Utrilla, S. Uzzi, M. Vailant, G. Valentini, V. Valette, A. van Elteren, E. Van Hemelryck, M. van Leeuwen, M. Vaschetto, A. Vecchiatto, J. Veljanoski, Y. Viala, D. Vicente, S. Vogt, C. von Essen, H. Voss, V. Votruba, S. Voutsinas, G. Walmsley, M. Weiler, O. Wertz, T. Wevers, L. Wyrzykowski, A. Yoldas, M. Žerjal, H. Ziaeeppour, J. Zorec, S. Zschocke, S. Zucker, C. Zurbach, and T. Zwitter, *Astronomy & Astrophysics* **616**, A1 (2018), [arXiv:1804.09365](https://arxiv.org/abs/1804.09365) [[astro-ph.GA](#)].
- [44] C. A. L. Bailer-Jones, J. Rybizki, M. Fouesneau, G. Mantelet, and R. Andrae, *The Astronomical Journal* **156**, 58 (2018), [arXiv:1804.10121](https://arxiv.org/abs/1804.10121) [[astro-ph.SR](#)].
- [45] J. Antoniadis, (2020), [arXiv:2011.08075](https://arxiv.org/abs/2011.08075) [[astro-ph.HE](#)].
- [46] F. Coti Zelati, D. F. Torres, J. Li, and D. Viganò, *Monthly Notices of the Royal Astronomical Society* **492**, 1025 (2020), [arXiv:1912.03953](https://arxiv.org/abs/1912.03953) [[astro-ph.HE](#)].
- [47] D. F. Torres, D. Viganò, F. Coti Zelati, and J. Li, *Monthly Notices of the Royal Astronomical Society* **489**, 5494 (2019), [arXiv:1908.11574](https://arxiv.org/abs/1908.11574) [[astro-ph.HE](#)].
- [48] T. J. Maccarone, M. A. P. Torres, C. T. Britt, S. Greiss, R. I. Hynes, P. G. Jonker, D. Steeghs, R. Wijnands, and G. Nelemans, *Monthly Notices of the Royal Astronomical Society* **426**, 3057 (2012), [arXiv:1207.5915](https://arxiv.org/abs/1207.5915) [[astro-ph.GA](#)].
- [49] S. Henleywillis, A. M. Cool, D. Haggard, C. Heinke, P. Callanan, and Y. Zhao, *Monthly Notices of the Royal Astronomical Society* **479**, 2834 (2018), [arXiv:1803.04822](https://arxiv.org/abs/1803.04822) [[astro-ph.HE](#)].
- [50] S. Dai, S. Johnston, M. Kerr, F. o. Camilo, A. Cameron, L. Toomey, and H. Kumamoto, *Astrophys. J. Letters* **888**, L18 (2020), [arXiv:1912.08079](https://arxiv.org/abs/1912.08079) [[astro-ph.HE](#)].
- [51] D. R. Lorimer, A. J. Faulkner, A. G. Lyne, R. N. Manchester, M. Kramer, M. A. McLaughlin, G. Hobbs, A. Posenti, I. H. Stairs, F. Camilo, M. Burgay, N. D'Amico, A. Corongiu, and F. Crawford, *Monthly Notices of the Royal Astronomical Society* **372**, 777 (2006), [arXiv:astro-ph/0607640](https://arxiv.org/abs/astro-ph/0607640) [[astro-ph](#)].
- [52] F. J. Kerr and D. Lynden-Bell, *Monthly Notices of the Royal Astronomical Society* **221**, 1023 (1986).
- [53] M. Ackermann, M. Ajello, W. B. Atwood, L. Baldini, J. Ballet, G. Barbiellini, D. Bastieri, K. Bechtol, R. Bellazzini, B. Berenji, R. D. Blandford, E. D. Bloom, E. Bonamente, A. W. Borgland, T. J. Brandt, J. Bregeon, M. Brigida, P. Bruel, R. Buehler, S. Buson, G. A.

- Caliandro, R. A. Cameron, P. A. Caraveo, E. Cavaz-
zuti, C. Cecchi, E. Charles, A. Chekhtman, J. Chi-
ang, S. Ciprini, R. Claus, J. Cohen-Tanugi, J. Conrad,
S. Cutini, A. de Angelis, F. de Palma, C. D. Dermer,
S. W. Digel, E. d. C. e. Silva, P. S. Drell, A. Drlica-
Wagner, L. Falletti, C. Favuzzi, S. J. Fegan, E. C. Fer-
rara, W. B. Focke, P. Fortin, Y. Fukazawa, S. Funk,
P. Fusco, D. Gaggero, F. Gargano, S. Germani, N. Gigli-
etto, F. Giordano, M. Giroletti, T. Glanzman, G. God-
frey, J. E. Grove, S. Guiriec, M. Gustafsson, D. Hadasch,
Y. Hanabata, A. K. Harding, M. Hayashida, E. Hays,
D. Horan, X. Hou, R. E. Hughes, G. Jóhannesson,
A. S. Johnson, R. P. Johnson, T. Kamae, H. Katagiri,
J. Kataoka, J. Knödseder, M. Kuss, J. Lande, L. La-
tronico, S. H. Lee, M. Lemoine-Goumard, F. Longo,
F. Loparco, B. Lott, M. N. Lovellette, P. Lubrano, M. N.
Mazziotta, J. E. McEnery, P. F. Michelson, W. Mitthum-
siri, T. Mizuno, C. Monte, M. E. Monzani, A. Morselli,
I. V. Moskalenko, S. Murgia, M. Naumann-Godo, J. P.
Norris, E. Nuss, T. Ohsugi, A. Okumura, N. Omodei,
E. Orlando, J. F. Ormes, D. Paneque, J. H. Panetta,
D. Parent, M. Pesce-Rollins, M. Pierbattista, F. Piron,
G. Pivato, T. A. Porter, S. Rainò, R. Rando, M. Razzano,
S. Razzaque, A. Reimer, O. Reimer, H. F. W. Sadrozin-
ski, C. Sgrò, E. J. Siskind, G. Spandre, P. Spinelli, A. W.
Strong, D. J. Suson, H. Takahashi, T. Tanaka, J. G.
Thayer, J. B. Thayer, D. J. Thompson, L. Tibaldo,
M. Tinivella, D. F. Torres, G. Tosti, E. Troja, T. L.
Usher, J. Vandenbroucke, V. Vasileiou, G. Vianello,
V. Vitale, A. P. Waite, P. Wang, B. L. Winer, K. S.
Wood, M. Wood, Z. Yang, M. Ziegler, and S. Zimmer, *As-
trophys. J.* **750**, 3 (2012), [arXiv:1202.4039 \[astro-ph.HE\]](#).
- [54] J.-M. Casandjian, *Astrophys. J.* **806**, 240 (2015),
[arXiv:1506.00047 \[astro-ph.HE\]](#).
- [55] D. J. Schlegel, D. P. Finkbeiner, and M. Davis, *Astro-
phys. J.* **500**, 525 (1998), [arXiv:astro-ph/9710327 \[astro-
ph\]](#).

Appendix A: Details of the Galactic MSP population

The MSP disk population. Disk MSPs may represent an important background for MSP bulge searches. For the disk population, we use a ‘‘Lorimer-disk’’ profile [51] whose number density is given by:

$$n(r, z) = \frac{NC^{B+2}}{4\pi R_\odot^2 z_s e^C \Gamma(B+2)} \left(\frac{r}{R_\odot}\right)^B \times \exp\left(-C\left(\frac{r-R_\odot}{R_\odot}\right)\right) \exp\left(-\frac{|z|}{z_s}\right), \quad (\text{A1})$$

with best-fit parameters $B = 3.91$, $C = 7.54$, defining the vertical and radial profile, and $z_s = 0.76$ pc the scale height [23]. N is the normalisation of the source density distribution, which is set by the total number of sources, while R_\odot is the Solar distance from the Galactic center, set to 8.5 kpc [52]. The best model for the (0.1 – 100 GeV) γ -ray luminosity function (GLF) of disk MSPs was found to be a broken power law [23]:

$$\frac{dN}{dL} \propto \begin{cases} L^{-\alpha_1} & L \leq L_b \\ L_b^{\alpha_2 - \alpha_1} L^{-\alpha_2} & L > L_b \end{cases} \quad (\text{A2})$$

with $\alpha_1 = 0.97$, $\alpha_2 = 2.60$ and $L_b = 10^{33.24}$ erg/s. From the estimated best-fit average disk luminosity, we can compute the total number of disk MSPs, see Tab. I.

The MSP bulge population. The MSP bulge population is made of two components: The boxy bulge (BB) and the nuclear bulge (NB). The BB number density is proportional to $K_0(r_s)$ with K_0 being the modified Bessel function of the second kind, with r_s given by:

$$r_s = \left[\left[\left(\frac{x}{x_0}\right)^2 + \left(\frac{y}{y_0}\right)^2 \right]^2 + \left(\frac{z}{z_0}\right)^4 \right]^{\frac{1}{4}},$$

and with $x_0 = 0.69$ kpc, $y_0 = 0.29$ kpc and $z_0 = 0.27$ kpc [25]. Here, (x, y, z) refer to the Cartesian BB coordinates system. The z axis is perpendicular to the Galactic plane and the x axis is rotated $\theta = 29.4^\circ$ away from the Galactic center-Sun axis in the clockwise direction [25]. The BB extends approximately from 30° to -20° in longitude and from -20° to 20° in latitude.

The NB [26], in turn, gets contributions from the nuclear stellar cluster (NSC) and the nuclear stellar disk (NSD). For the NSD, the mass density in cylindrical coordinates is given by:

$$\rho^{\text{NSD}}(r, z) = \begin{cases} \rho_0^{\text{NSD}} \left(\frac{r}{1 \text{ pc}}\right)^{-0.1} e^{-\frac{|z|}{45 \text{ pc}}} & r \leq 120 \text{ pc} \\ \rho_1^{\text{NSD}} \left(\frac{r}{1 \text{ pc}}\right)^{-3.5} e^{-\frac{|z|}{45 \text{ pc}}} & 120 \text{ pc} < r \leq 220 \text{ pc} \\ \rho_2^{\text{NSD}} \left(\frac{r}{1 \text{ pc}}\right)^{-10} e^{-\frac{|z|}{45 \text{ pc}}} & r > 220 \text{ pc} \end{cases} \quad (\text{A3})$$

with $\rho_0^{\text{NSD}} = 301 M_\odot \text{ pc}^{-3}$ such that the mass within 120 pc is $8 \times 10^8 M_\odot$. ρ_1^{NSD} and ρ_2^{NSD} are determined such to

give a continuous NSD mass profile. The NSD is located between $|l| < 2^\circ$ and $|b| < 2^\circ$. For the NSC, the mass density in spherical coordinates is given by:

$$\rho^{\text{NSC}}(r) = \begin{cases} \frac{\rho_0^{\text{NSC}}}{1 + \left(\frac{r}{r_0}\right)^2} & r \leq 6 \text{ pc} \\ \frac{\rho_1^{\text{NSC}}}{1 + \left(\frac{r}{r_0}\right)^3} & 6 \text{ pc} < r \leq 200 \text{ pc} \\ 0 & r > 200 \text{ pc} \end{cases} \quad (\text{A4})$$

with $r_0 = 0.22$ pc and $\rho_0^{\text{NSC}} = 3.3 \times 10^6 M_\odot \text{ pc}^{-3}$. ρ_1^{NSC} is determined such to give a continuous NSC mass profile. The NSC is contained in the innermost $2^\circ \times 2^\circ$. We assume the GLF of BB and NB MSPs to be the same as in the disk. Together with estimations of the average luminosity $\langle L_\gamma^{\text{obs}} \rangle$ [8], the GLF allows us to compute the total number of bulge MSPs for the different bulge components. We quote those numbers in Tab. I, and show the spatial distribution of the MSP source density in Fig. 4.

TABLE I. Observed or estimated average γ -ray luminosity $\langle L_\gamma^{\text{obs}} \rangle$ [8, 23] for the Galactic MSP population components, together with the derived total number of MSPs in each component, N_{tot} .

	$\langle L_\gamma^{\text{obs}} \rangle$ [erg/s]	N_{tot}
BB	1.73×10^{37}	27674
NSD	1.63×10^{36}	2606
NSC	5.89×10^{34}	94
Disk	1.5×10^{37}	24009

Appendix B: Testing Monte Carlo systematics

γ -ray luminosity function for the bulge. Since current γ -ray data are not sensitive to the detection of individual MSPs in the Galactic bulge, it is difficult to robustly constrain the GLF of bulge MSPs. Although the GLF of the putative MSPs in the Galactic bulge has been found to be consistent with that characterizing resolved disk MSPs [27], we cannot exclude that the GLF of bulge MSPs differs from the disk one. We here test this possibility and the impact that a variation of the bulge GLF can have on X-ray sensitivity prospects. We vary the parameters of our baseline GLF around their best-fit values [23], but beyond the statistical 1σ errors, and we check *a posteriori* that the number of detectable γ -ray bulge MSPs for that variation is still in agreement with findings from [23], i.e. a few detectable γ -ray bulge MSPs (adopting the *Fermi*-LAT detection sensitivity model as in [23]). Thoroughly exploring γ -ray implications for more extreme variations of the bulge GLF is beyond the scope of the present work. In Fig. 5, we show how the number of detectable sources changes under exemplary variations of the bulge GLF parameters. By varying α_1 ,

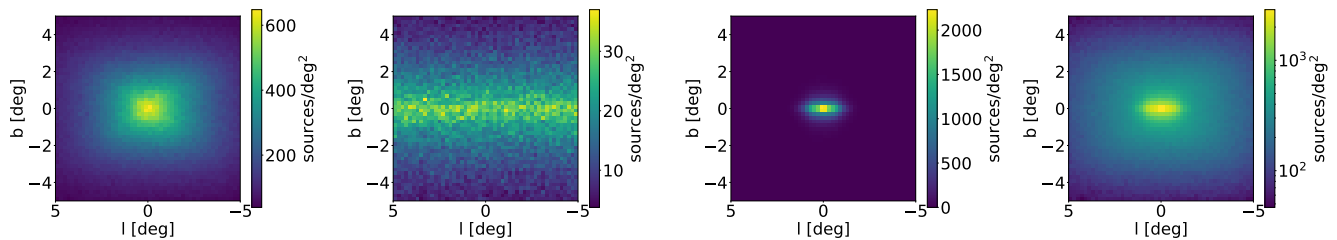


FIG. 4. From left to right, source density of the MSP Galactic population for the BB, disk and NB components, and their sum.

α_2 , and L_b (see Eq. A2) one at the time, we find that the number of detectable X-ray sources is mildly affected by changes of the γ -ray modeling.

Examples of variations that we can get are presented in Fig. 5: With respect to the baseline prediction of 95 ± 9 detectable MSPs, we get 102 ± 10 detectable sources for $\alpha_1 = -0.97$, 84 ± 9 for $\alpha_2 = 2.4$ (averages performed over 100 Monte Carlo simulations), and 79 ± 9 for $L_b = 10^{32.8}$ erg/s (average performed over 40 Monte Carlo simulations).

The reason why X-ray predictions are not too sensitive to the bulge GLF lies in the fact that the largest fraction of detectable X-ray MSPs has γ -ray fluxes close to the best-fit L_b value, and, therefore, we need very extreme variations of the parameters to induce a sizeable effect on the number of detectable X-ray MSPs. Such variations, however, are not allowed if we require consistency with γ -ray (non-)detection of individual bulge MSPs.

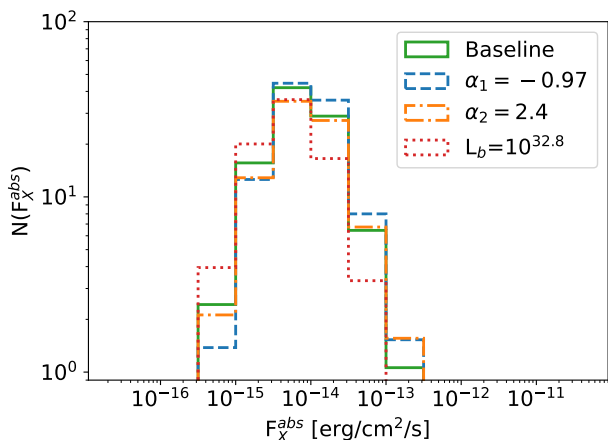


FIG. 5. X-ray energy flux distribution (0.5 – 7 keV) of detectable MSPs, averaged over 100 Monte Carlo simulations (40 for the red dotted histogram), for illustrative variations of the bulge GLF parameters. Here, L_b is expressed in units of erg/s.

Modeling X-ray Galactic absorption. For the baseline model of total hydrogen in the Galaxy, we use the gas maps publicly available at <https://github.com/>

[chrisgordon1/galactic_bulge](#). The maps are split in four concentric rings, separated by $R = 3.5, 8$ and 10 kpc. We take the hydrogen-to-CO conversion factor partially from [9], using $X_{CO} = 0.4 (1.0) \times 10^{20} \text{ cm}^{-2}/(\text{K km s}^{-1})$ for $R \leq 3.5$ kpc ($3.5 \text{ kpc} < R \leq 8.0$ kpc). The outer rings ($R > 8$ kpc) X_{CO} being poorly or completely unconstrained by [9], we adopt the standard reference value of $1.9 \times 10^{20} \text{ cm}^{-2}/(\text{K km s}^{-1})$ [53]. We add the contribution from dark gas by including the dust-to-gas residual reddening maps from [9]. To convert E(B-V) residual maps in units of hydrogen column density we use a dust-to-gas ratio $X_{\text{dust}} = 41.4 \times 10^{20} \text{ cm}^{-2} \text{ mag}^{-1}$ [54].

To explore the systematic uncertainty due to the modeling of the total hydrogen in the Galaxy and its distribution along the line of sight, we consider two additional models for Galactic hydrogen column density. First, we use the `dustmaps` Python module¹, which implements the 2D extinction map from [55]. Being a 2D map, no distance information can be retrieved, and the absorption towards a given MSP may be overestimated. Using 2D dust map should provide a lower limit on the number of detectable MSPs. Secondly, we consider a model with no absorption by setting $N_H = 0 \text{ cm}^{-2}$. In this extreme case, on the contrary, we grossly underestimate the absorption and get an upper limit on the number of detectable MSPs. In particular, we obtain 75 ± 8 detectable MSPs for the 2D dust map, and 267 ± 15 for the unabsorbed case (averages over 100 Monte Carlo simulations). We show these results in Fig. 6. Uncertainties in the Galactic hydrogen modeling therefore should not diminish the final X-ray predictions by more than 20%, while any enhancement is *theoretically* bound to be within a factor 2.8 of our benchmark.

Notice that any change in the modeling of the synthetic population would also affect the Monte-Carlo-based cuts for flux ratios and band fractions, and, therefore, the final source selection. We do expect, however, that the number of CSC selected candidates would not be significantly altered by changes in the MSP modeling, given the reduced impact it has on the number of detectable synthetic sources.

¹ <https://dustmaps.readthedocs.io/en/latest/>.

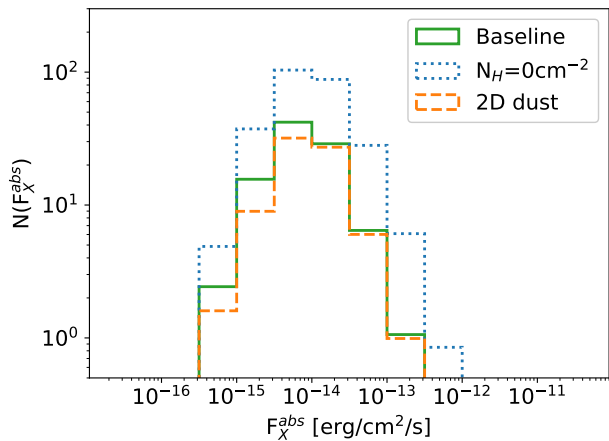


FIG. 6. As in Fig. 5, showing variations due to the modeling of Galactic hydrogen column density (see text for details).

Appendix C: *Chandra* limiting sensitivity maps

In Fig. 7, we show the sensitivity map of ACIS for the TRUE and MARGINAL detection likelihood classes, as defined at <https://cxc.harvard.edu/csc/columns/stack.html>. All predictions in the main text refer to this ACIS (0.5 – 7 keV) sensitivity map, for both Monte Carlo and *Chandra* catalog. Indeed, CSC source detection is not based on likelihoods derived from Poisson fluctuations, like those used to build the sensitivity maps. Therefore, for a meaningful comparison between Monte Carlo and catalog we should apply the sensitivity cut also to CSC sources, see “Limiting Sensitivity” at <https://cxc.harvard.edu/csc/char.html>, and https://cxc.harvard.edu/csc/memos/files/Primini_limiting-sensitivity.pdf.

In Fig. 8, we provide Monte Carlo predictions and minimal CSC selection obtained by using the sensitivity map corresponding only to the TRUE detection likelihood class.

In this case, we get 54 ± 7 detectable MSPs (vs. 95 ± 9 for the baseline scenario), and 4703 source in the minimal CSC selection (vs. 6918). The variation induced by the use of a more restrictive sensitivity map is no more than a factor of two, affect similarly the signal and the background.

Appendix D: S/N spatial optimization

By exploiting the source spatial distribution, one could in principle improve the constraining power of the analysis. The synthetic bulge MSP population has a specific distribution in space which traces the BB and the NB. Footprints of such a distribution are left in the l

and b profiles of detectable MSPs. In Fig. 9 (left panel), we show the 2D (l , b) histogram of detectable MSPs.

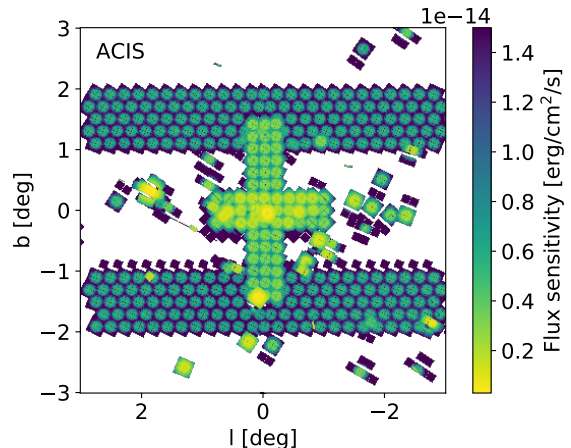


FIG. 7. ACIS limiting sensitivity map for the TRUE and MARGINAL detection likelihood classes.

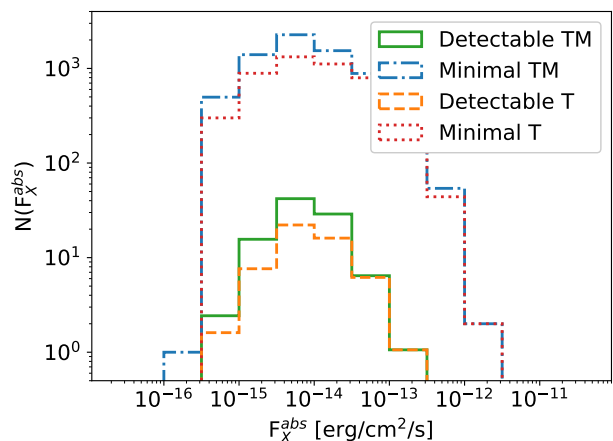


FIG. 8. As in Fig. 3, here displaying the number of detectable MSPs and *Chandra* minimally selected sources for the baseline sensitivity map (TRUE+MARGINAL) and for the TRUE detection likelihood class limiting sensitivity.

where a clear “cusp” about the Galactic center direction can be seen. On the other hand, we do expect CSC selected sources not to strictly follow the same distribution, given the contamination from other source classes, see Fig. 9 (central panel). Ideally, maximizing the ratio of detectable-to-candidate MSPs (Fig. 9, right panel) one can optimize the ROI and design a strategy to further cut down the candidates’ sample. As discussed in the main text, this approach would however require to model the MSP spatial distribution on small scales, a goal which cannot be reliably achieved based on current γ -ray analyses and/or theoretical models.

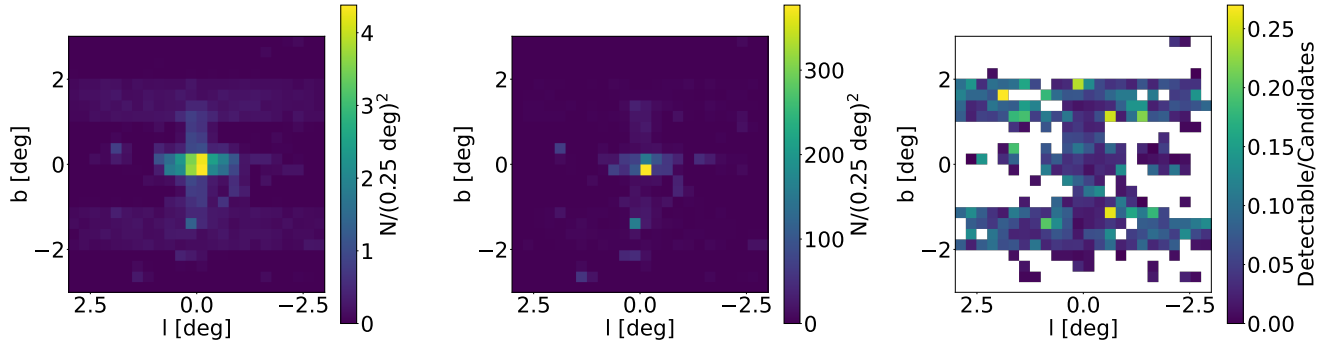


FIG. 9. **Left panel:** 2D (l , b) histogram of detectable MSPs, averaged over 100 Monte Carlo simulations. **Central panel:** Same as left panel for the 2981 objects of the conservative selection. **Right panel:** Detectable-to-candidate MSPs ratio.